PHYSICAL REVIEW B **67**, 045321 (2003)

Microscopic mapping of strain relaxation in uncoalesced pendeoepitaxial GaN on SiC

U. T. Schwarz*
Faculty of Physics, Regensburg University, D-93040 Regensburg, Germany

P. J. Schuck, M. D. Mason, and R. D. Grober
Yale University, Applied Physics, Becton Center, New Haven, Connecticut 06520

A. M. Roskowski, S. Einfeldt, and R. F. Davis
North Carolina State University, Raleigh, North Carolina 27695

(Received 28 August 2002; published 30 January 2003)

Mapping of the strain distribution in uncoalesced pendeoepitaxial GaN on SiC by spatially resolved micro-Raman and microphotoluminescence, and lattice constants measured by high-resolution x-ray diffraction provide a consistent picture of relaxation of inhomogeneous and anisotropic strain. The pendeoepitaxial wings show a nearly complete strain relaxation and high optical quality with extremely narrow donor bound exciton peaks. The narrow exciton linewidths result in the determination of *c*-axis strain to an accuracy of 6×10^{-6}.

DOI: 10.1103/PhysRevB.67.045321 PACS number(s): 68.60.Bs, 78.55.Cr, 78.30.Fs, 78.66.Db

Pendeoepitaxy is a technique of epitaxial overgrowth that produces GaN epilayers with low defect densities as an interesting substrate for optoelectronic devices in the blue to ultraviolet spectral region.[1–3] Maskless pendeoepitaxial GaN samples consist of alternating regions of GaN stripes, grown on the substrate, and free-hanging GaN wings, which grow laterally from the sides of the stripes but make no contact with the substrate or to a mask. Strain induced by lattice mismatch, dislocations, and disparate thermal expansion coefficients between GaN and the substrate therefore is expected to be greatly reduced in the free-hanging wing regions. To characterize the different properties of wing and stripe regions and study the microscopic origin of strain, spatially resolved experiments are needed. Microphotoluminescence (μ-PL), cathodoluminescence (CL), and micro-Raman (μ-Raman) have previously been used to study inhomogeneous strain and free-carrier distribution in epitaxial laterally overgrown (ELOG) GaN.[3,4] We use μ-Raman and μ-PL to create images that map strain by tracking frequency shifts of the E_2 (high) phonon mode and free or bound exciton lines in uncoalesced pendeoepitaxial GaN on SiC. With diffraction limited spatial resolution of 0.7 μm for μ-Raman and 0.4 μm for μ-PL,[5] we measure a relaxation of strain from stripe to wings as well as the homogeneity of strain within the wings. Absolute lattice constants were measured separately for the stripe and wing regions by high-resolution x-ray diffraction (HRXRD). A comparison of these experiments provides a consistent picture of strain relaxation mechanisms. We demonstrate that the wings consist of domains of homogeneous strain with characteristic lengths of 2–5 μm. These domains show neutral donor bound exciton (D^0X) peaks with linewidths smaller than 0.3 meV and presumably have low defect densities.

Our data are acquired using a scanning confocal UV microscope with 100× magnification. All measurements are performed at low temperature ($T=8$ K) with the sample mounted on a coldfinger inside a liquid-helium, continuous-flow Janis microscope cryostat. The 325-nm line of a He-Cd laser is used for PL excitation while the 488-nm line from an argon-ion laser is used as the Raman pump. We both excite and collect through a 0.75-NA, 63× Zeiss microscope objective that corrects for the spherical aberration encountered when passing through a quartz window above the sample. Collected emission is focused through a 40-μm pinhole, defining our spatial resolution, and dispersed with a 2400-lines/mm grating by a 1-m monochromator. The spectra are detected with a liquid-nitrogen-cooled charge-coupled device (CCD) camera.

A cross section of the uncoalesced pendeoepitaxial structure is shown in Fig. 1. Stripes oriented along the $[1\bar{1}00]$ direction were etched from a 1-μm GaN epilayer grown by metalorganic vapor phase epitaxy (MOVPE) on 6H SiC (0001) using a 0.1-μm AlN buffer layer. In a second growth step the wing-stripe-wing structure is formed. Details of the growth process can be found elsewhere.[6] In this work, the *x-y* plane is defined to be parallel to the sample surface with the *x* axis directed perpendicular to the stripe orientation (and parallel to the lateral direction of growth).

The position of the nonpolar E_2 (high) phonon mode is a sensitive indicator for strain.[8] Figure 2(a) shows a map of the Raman frequency of the E_2 (high) phonon in a density plot. Raman measurements were carried out at low temperature ($T=8$ K) in backscattering geometry. Lower E_2 (high) phonon frequencies (dark areas) correspond to high tensile strain

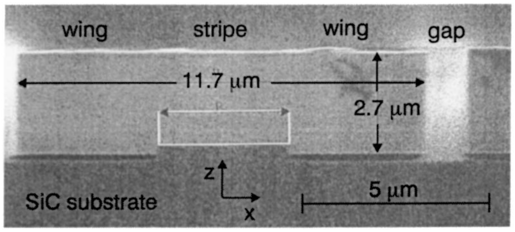

FIG. 1. Scanning electron microscopy cross-sectional images of uncoalesced pendeoepitaxy GaN. The white rectangle marks the original GaN stripe before the overgrowth process.

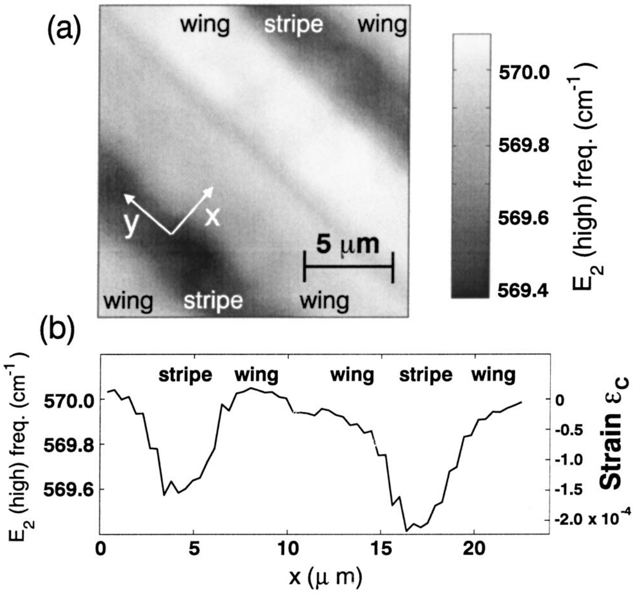

FIG. 2. (a) Gray scale density plan-view maps of the Raman frequency shift of the E_2 (high) phonon. Dark areas correspond to low frequency and high tensile strain in the c plane. Wing and stripe regions in this top view are marked in accordance with the side view in Fig. 1. (b) Frequency of the E_2 (high) phonon along a line in x direction perpendicular to the stripes.

in the x-y plane in the stripe regions, induced by the 6H SiC substrate. In the wing regions, relaxation of this strain causes an upshift of the E_2 (high) frequency (bright areas).

Figure 2(b) shows the frequency of the E_2 (high) Raman mode as a function of position along a line in the x direction. The absolute frequencies measured in the wing regions agree with those listed in Ref. 7 for relaxed GaN. For a quantitative evaluation and comparison with HRXRD results we use the linear relation for strain along the c axis $\varepsilon_c=\Delta c/c=3.8\times10^{-4}$ cm $\Delta\Omega$, where the E_2 (high) mode shift $\Delta\Omega$ is caused by biaxial strain in the x-y plane.[8] The strain in the stripe, relative to the wing, is $\varepsilon_c=-(1.7\pm0.5)\times10^{-4}$. The typical linewidth of the E_2 (high) mode is 3 cm^{-1}, and our smallest detectable frequency shift is 0.2 cm^{-1} corresponding to a strain of $e_c=7\times10^{-5}$. This is too large to resolve strain variations within the wings.

In HRXRD, the reciprocal space maps around the GaN (002) reflection recorded with the diffraction plane perpendicular to the stripe direction allow one to measure lattice constants of the stripe and wings (see Table I). The compressive strain along the c axis, $\varepsilon_c=-(1.6\pm0.2)\times10^{-4}$, calculated from these lattice constants is consistent with the strain, $\varepsilon_c=-(1.7\pm0.5)\times10^{-4}$, derived from the μ-Raman measurement.

TABLE I. Lattice parameters measured by HRXRD at room temperature. The strain was calculated from the lattice constants as $\epsilon_c=(c_{\text{stripe}}-c_{\text{wing}})/c_{\text{wing}}$.

c (wing) [Å]	5.18859 ± 0.00005
c (stripe) [Å]	5.18775 ± 0.00006
ϵ_c (HRXRD)	$-(1.6\pm0.2)\times10^{-4}$
ϵ_c (Raman)	$-(1.7\pm0.5)\times10^{-4}$
ϵ_c (PL)	-3×10^{-4}

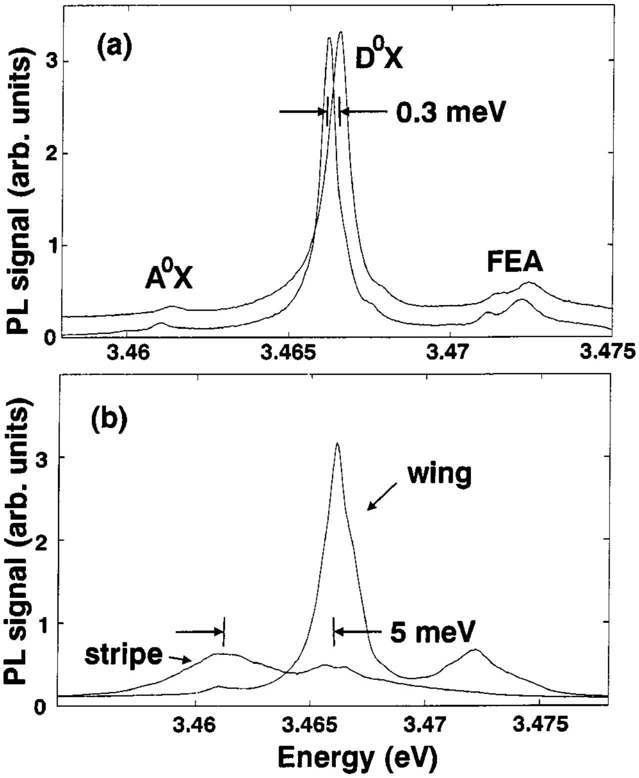

FIG. 3. (a) μ-PL spectra at two spots in the wing region of uncoalesced pendeoepitaxial GaN. (b) PL spectra integrated over $1.5\times18\ \mu\text{m}^2$ in the stripe and $6\times18\ \mu\text{m}^2$ in the wing regions, respectively. Broadening and downshift is due to inhomogeneous strain. A^0X, D^0X, and FEA refer to neutral acceptor bound, neutral donor bound, and free A excitonic transitions, respectively.

Figure 3 shows near band-edge photoluminescence spectra. The power density of the laser excitation is approximately 10 W/cm^2. The two spectra in Fig. 3(a) were taken in the wing region at two distinct locations. The most prominent feature is the D^0X line at ~3.466 eV. The extremely narrow D^0X linewidth of less than 0.3 meV is in the range of the lowest values reported for homoepitaxial GaN.[9,10] The two other prominent features are the neutral acceptor bound exciton (A^0X) at ~3.461 eV and the free A exciton (FEA) at ~3.472 eV.

The narrow linewidth of the D^0X peak makes it possible to detect peak spectral shifts down to 0.1 meV. Using a linear relation $\varepsilon_c=(59\pm6)\times10^{-6}$ meV^{-1} ΔE for the D^0X peak shift by biaxial strain,[8] this corresponds to a detectable strain $\varepsilon_c=6\times10^{-6}$. This is an order of magnitude increase in sensitivity compared to the Raman method. In Fig. 3(a), all features in the two spectra are shifted against each other by 0.3 meV. The strain associated with this shift is $\varepsilon_c=1.8\times10^{-5}$.

The two PL spectra in Fig. 3(b) were averaged over $1.5\times18\ \mu\text{m}^2$ and $6\times18\ \mu\text{m}^2$ in the stripe and wing regions, respectively. The D^0X peak in the wing region is slightly broadened because regions of different strain are probed. The

D^0X and FEA features in the stripe spectra are downshifted by approximately 5 meV and extremely broadened relative to the wing spectral features. This large downshift corresponds to a compressive strain along the c axis of $\varepsilon_c = -3\times10^{-4}$, which is a factor of 2 different than our μ-Raman results. We comment on this difference in the following paragraph. The observed broadening of the D^0X line indicates inhomogeneous strain in the stripe that is most likely related to the high density of threading dislocations in this region.[1]

The picture of biaxial tensile strain in the x-y plane, which is induced by the SiC substrate in the stripe and is relaxed in the wings, might be too simple. The wings can relieve strain predominantly in the x-axis direction perpendicular to the stripes. In contrast, the strain cannot relax in the y-axis direction because the GaN is a compact film along the stripes. We have observed this anisotropic strain relaxation by HRXRD in all pendeoepitaxial GaN on SiC. It would call for a treatment of strain-induced E_2 (high) and D^0X shifts in a deformation potential model.[11] However, the error margins of the indicated potential constants are too large for a meaningful distinction of the uniaxial and biaxial a-axis strain from Raman and PL shifts. We attribute the different absolute values of ε_c measured by μ-PL, μ-Raman, and HRXRD partially to this anisotropic strain. As a further complication, different concentrations of point defects in the stripe and wings caused by the growth process can contribute inhomogeneous tensile hydrostatic strain.[8] Moreover, it should be emphasized that μ-Raman probes the entire GaN film thickness whereas μ-PL is sensitive only to the material near the surface. Therefore another cause for the different values of ε_c can be an inhomogeneous strain in the z direction (c axis). The larger value $\varepsilon_c = -3\times10^{-4}$ measured by μ-PL indicates a larger biaxial tensile strain in the x-y plane near the surface of the stripe.

Figure 4 shows monochromatic maps of the relative photoluminescence intensity at different energies for uncoalesced pendeoepitaxial GaN. All four maps stem from one $18\times18\ \mu\text{m}^2$ scan, where an entire PL spectrum was collected at each point in the scan. As is shown in Fig. 4(a), the stripe is brightest at low energies due to the broad spectral hump around 3.462 eV [see spectrum in Fig. 3(b)]. Figures 4(b)–(d) show intensity distributions at energies of 3.4652, 3.4664, and 3.4676 eV, respectively. Each of these energies corresponds to the center frequency of the D^0X transition in three separate regions of different strain. It should be noted that Figs. 4(a)–(d) have different gray scales. Discrete domains of uniform D^0X energy are visible in Figs. 4(b)–(d). These domains have characteristic lengths of 2–5 μm and are limited to the wing regions. It is important to note that the D^0X energy changes abruptly, i.e., it is constant for a few micrometers and then changes over a distance comparable to the optical resolution of our instrumental setup which is 0.4 μm. The energy difference $\Delta E = 1.2$ meV between Figs. 4(b) and (c) and 4(c) and (d) corresponds to a strain difference as small as $\varepsilon_c = 7.1\times10^{-5}$.

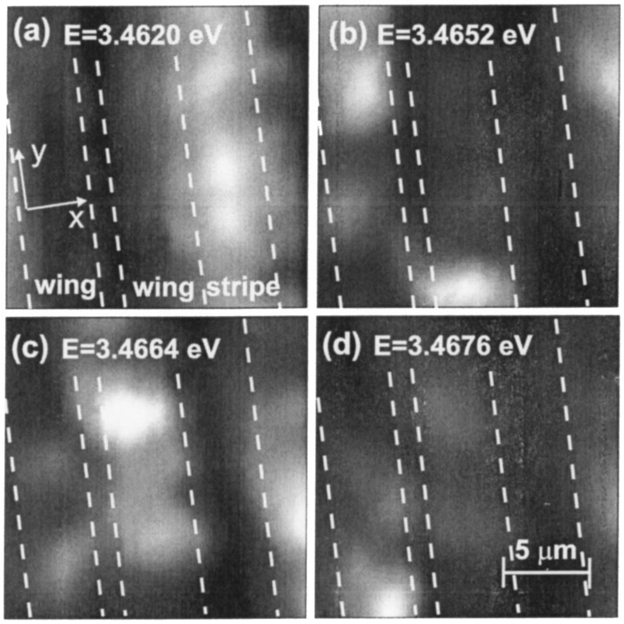

FIG. 4. Gray scale density plan-view maps of the PL intensity over an energy range of 0.4 meV at the indicated energies. Each of the indicated energies corresponds to the center frequency of the D0X transition in four separate regions of different strain. The linear grayscales for (a)–(d) are as follows: (a) black $=0.2\,I_0$, white $=I_0$; (b) black $=0.5\,I_0$, white $=7.6\,I_0$; (c) black $=0.7\,I_0$, white $=11.9\,I_0$; (d) black $=0.4\,I_0$, white $=3.5\,I_0$ where $I_0 =$ maximum intensity in (a).

As seen in Fig. 4, the domains in the PL maps exhibit D^0X energy constant to better than 0.3 meV. We believe this indicates domains of uniform strain. This observation is consistent with the generation of strain and accumulation of threading dislocations at grain boundaries by island coalescence, which has been demonstrated for GaN films on sapphire.[12]

In summary, the high sensitivity and spatial resolution of μ-PL allows the mapping of residual strain in the nearly relaxed wing regions. μ-Raman, μ-PL, and HRXRD measurements consistently show the relaxation of strain from stripe to wings. Differences in the absolute values of measured strain for the different experiments were attributed to an inhomogeneous and anisotropic relaxation of strain, which was discussed in terms of the geometry of the pedeoepitaxial structure and possible hydrostatic strain caused by point defects. Our experiments show that μ-Raman allows for measurements in highly inhomogeneously strained material. μ-PL on the other hand is sensitive enough to reveal domains of homogeneous strain within the wings. The linewidth of the D^0X was smaller than 0.3 meV in the wing region, demonstrating the potential of pendeoepitaxy to produce high quality GaN.

The work at Yale is supported by the Office of Naval Research MURI on Polarization Electronics Contract No. N00014-96-1-1179, under the direction of Dr. Colin E. C. Wood.

---

[*] Electronic address: uli.schwarz@physik.uni-regensburg.de

[1] T. Zheleva, S. Smith, D. Thomson, K. Linthicum, P. Rajagopal, and R. F. Davis, J. Electron. Mater. **28**, L5 (1999).

[2] P. Fini, H. Marchand, J. P. Ibbetson, B. Moran, L. Zhao, S. P. DenBaars, J. S. Speck, and U. K. Mishra, in *Wide-Bandgap Semiconductors for High-Power, High-Frequency and High-Temperature Applications–1999*, edited by S. Binari, A. Burk, M. Mellock, and C. Nguyen, Mater. Res. Soc. Symp. Proc. No. **572** (Materials Research Society, Pittsburgh, 1999), p. 315.

[3] A. Strittmatter, S. Rodt, L. Reissmann, D. Bimberg, H. Schröder, E. Obermeier, T. Riemann, J. Christen, and A. Krost, Appl. Phys. Lett. **78**, 727 (2001).

[4] F. Bertram, T. Riemann, J. Christen, A. Kaschner, A. Hoffmann, C. Thomsen, K. Hiramatsu, T. Shibata, and N. Sawaki, Appl. Phys. Lett. **74**, 359 (1999).

[5] P. J. Schuck, M. D. Mason, R. D. Grober, O. Ambacher, A. P. Lima, C. Miskys, R. Dimitrov, and M. Stutzmann, Appl. Phys. Lett. **79**, 952 (2001).

[6] A. M. Roskowski, P. M. Miraglia, E. A. Preble, S. Einfeldt, T. Stiles, R. F. Davis, P. J. Schuck, R. D. Grober, and U. T. Schwarz, Phys. Status Solidi A **188**, 729 (2001).

[7] M. Giehler, M. Ramsteiner, P. Waltereit, O. Brandt, K. H. Ploog, and H. Obloh, J. Appl. Phys. **89**, 3634 (2001).

[8] C. Kisielowski, K. Krüger, S. Ruminov, T. Suski, J. W. Ager, III, E. Jones, Z. Liliental-Weber, M. Rubin, E. R. Weber, M. D. Bremser, and R. F. Davis, Phys. Rev. B **54**, 17 745 (1996).

[9] A. M. Roskowski, E. A. Preble, S. Einfeldt, P. M. Miraglia, and R. F. Davis, J. Electron. Mater. **31**, 421 (2002).

[10] C. R. Miskys, M. K. Kelly, O. Ambacher, G. Martinez-Criado, and M. Stutzmann, Appl. Phys. Lett. **77**, 1858 (2000).

[11] V. Yu. Davydov, N. S. Averkiev, I. N. Goncharuk, D. K. Nelson, I. P. Nikitina, A. S. Polkovnikov, A. N. Smirnov, M. A. Jacobson, and O. K. Semchinova, J. Appl. Phys. **82**, 5097 (1997).

[12] T. Böttcher, S. Einfeldt, S. Figge, R. Chierchia, H. Heinke, D. Hommel, and J. S. Speck, Appl. Phys. Lett. **78**, 1976 (2001).